

SCIENTIFIC REPORTS



OPEN

Intrinsic functional connectivity reduces after first-time exposure to short-term gravitational alterations induced by parabolic flight

Angelique Van Ombergen¹, Floris L. Wuyts¹, Ben Jeurissen², Jan Sijbers², Floris Vanhevel³, Steven Jillings¹, Paul M. Parizel³, Stefan Sunaert⁴, Paul H. Van de Heyning¹, Vincent Dousset⁵, Steven Laureys⁶ & Athena Demertzi^{6,7}

Spaceflight severely impacts the human body. However, little is known about how gravity and gravitational alterations affect the human brain. Here, we aimed at measuring the effects of acute exposure to gravity transitions. We exposed 28 naïve participants to repetitive alterations between normal, hyper- and microgravity induced by a parabolic flight (PF) and measured functional MRI connectivity changes. Scans were acquired before and after the PF. To mitigate motion sickness, PF participants received scopolamine prior to PF. To account for the scopolamine effects, 12 non-PF controls were scanned prior to and after scopolamine injection. Changes in functional connectivity were explored with the Intrinsic Connectivity Contrast (ICC). Seed-based analysis on the regions exhibiting localized changes was subsequently performed to understand the networks associated with the identified nodes. We found that the PF group was characterized by lower ICC scores in the right temporo-parietal junction (rTPJ), an area involved in multisensory integration and spatial tasks. The encompassed network revealed PF-related decreases in within- and inter-hemispheric anticorrelations between the rTPJ and the supramarginal gyri, indicating both altered vestibular and self-related functions. Our findings shed light on how the brain copes with gravity transitions, on gravity internalization and are relevant for the understanding of bodily self-consciousness.

Spaceflight induces several physiological changes in the human body, such as fluid shifts, neurovestibular disturbances, bone loss and muscle atrophy¹. Space crew adapt fairly well to these changes, depending on the site of action and the applied countermeasures. Yet, despite several decades of human spaceflight, countermeasures are not entirely successful. For example, space motion sickness is still present among several space travellers when arriving in the International Space Station, and upon return to Earth, orthostatic intolerance often occurs next to spatial disorientation, continued osteoporosis and muscle atrophy^{1,2}. Some space travellers adapt easier to the relatively hostile environment of space than others, and second - time fliers certainly experience fewer problems, which has been well described for e.g. space motion sickness².

The central nervous system also seems capable of adaptation to microgravity by the process of neuroplasticity, as previously shown in animals³⁻⁵. Yet, little is known about the effects of microgravity and gravity transitions on the human brain⁶. Recently, in a functional MRI study with a single cosmonaut, we showed that long-duration spaceflight induced functional changes in the right insula and in sensorimotor-cerebellar connectivity⁷.

¹Antwerp University Research Centre for Equilibrium and Aerospace (AUREA), University of Antwerp, Antwerp, Belgium. ²Vision Lab, Department of Physics, University of Antwerp, Antwerp, Belgium. ³Department of Radiology, Antwerp University Hospital & University of Antwerp, Antwerp, Belgium. ⁴KU Leuven – University of Leuven, Department of Imaging & Pathology, Translational MRI, Leuven, Belgium. ⁵University of Bordeaux, CHU de Bordeaux, INSERM Magendie, Bordeaux, France. ⁶Coma Science Group, GIGA-Research & Neurology Department, University and University Hospital of Liège, Liège, Belgium. ⁷Institut du Cerveau et de la Moelle Epinière - Brain and Spine Institute, Hôpital Pitié-Salpêtrière, Paris, France. Steven Laureys and Athena Demertzi contributed equally to this work. Correspondence and requests for materials should be addressed to F.L.W. (email: floris.wuyts@uantwerpen.be)

Received: 12 December 2016
Accepted: 26 April 2017
Published online: 08 June 2017

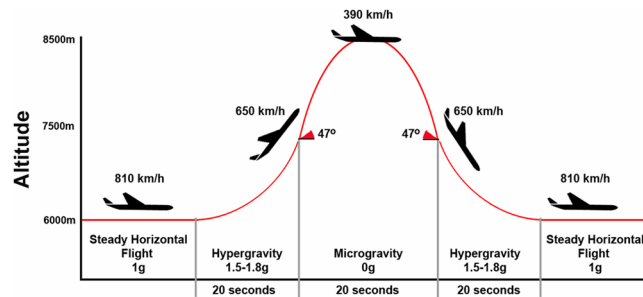


Figure 1. Flight trajectory during the parabolic manoeuvre.

However, research on humans in space is expensive and subject to several logistic and payload restrictions. Hence, ground-based models have been developed, in which some aspects of spaceflight can be simulated. Dry immersion⁸ and head-down bed rest⁹ mimic certain characteristics of spaceflight quite well, such as ‘supportlessness’ or fluid shifts respectively. Nevertheless, these space analogs are performed in the presence of a constant gravitational force, and therefore not suitable to study the impact of microgravity and acute gravitational transitions on the human brain.

Parabolic flight is a “ground-based” alternative, during which a specific parabolic trajectory is carried out, wherein the acceleration of the aircraft cancels the gravity acceleration. A hypergravity phase, characterized by 1.5–1.8 g lasting around 30–35 s, precedes and follows the microgravity phase. Microgravity resembles zero g and lasts around 20–25 s. In between parabolas, the aircraft flies in normal 1 g conditions¹⁰. The sensation of weightlessness is caused when the aircraft is in free fall, because during that time it does not exert any ground reaction force on its contents. Thus, PF consists of gravity transitions, (microgravity, hypergravity and normal gravity phases), generated during 31 parabolas. An entire flight lasts around 3 to 3.5 h (Fig. 1).

The aim of the present study was to measure the effects of acute exposure to gravitational transitions, induced by PF, in naïve human subjects. We hypothesized that a) after short-term exposure to gravity alterations the brain will show modifications at the functional level and b) these modifications will concern the vestibular system. Our first hypothesis is supported by previous fMRI studies showing changes in brain function after acute environmental modulations (e.g. refs 11–13) or after intense subjective experiences (e.g. refs 14 and 15), suggesting that short-term plasticity is measurable with neuroimaging tools. Our second hypothesis is based on the observations that, in normal conditions, vestibular cues give information on the pull of the gravito-inertial acceleration being the vector sum of gravity and all other linear accelerations exerted on the vestibulum. Together with somatosensory information from joints, skin and muscles, the vestibular information is integrated with allocentric information from the visual surroundings and egocentric cues about one’s own body axis¹⁶. During a PF, especially during the microgravity phase, the vestibular input is largely disturbed and therefore might cause an incongruity with the normal terrestrial expectations regarding verticality and spatial orientation¹⁷. As no previous neuroimaging investigations have been performed under these conditions^{6, 18, 19}, a data-driven approach was here implemented to investigate changes in fMRI functional connectivity during resting state. Functional connectivity refers to the temporal correlation between spatially remote neurophysiological events, expressed as a deviation from statistical independence in distributed brain regions²⁰. In order to better comprehend how the identified regions, which exhibit these changes, are related to the rest of the brain, we subsequently estimated the cerebral networks correlating with these nodes. In order to debrief overall functionality, subjective ratings on the level of wakefulness, emotional function and motion sickness were collected prior and after the PF.

Materials and Methods

Subjects. The inclusion criteria to participate in the PF were: adult participants, no previous participation in a PF, non-smokers, and good physical condition according to a complete medical check-up screening. Each selected subject participated in one PF only. Based on these criteria, an initial cohort of 31 volunteers was obtained. Three subjects were excluded from the analysis because post-flight fMRI data could not be obtained due to logistical reasons. The final PF cohort included 28 healthy participants (11 female; mean (SD) age 31 (7) years). Prior to the PF, all selected participants received scopolamine (0.25 mg/1 mL; 0.7 mL for males and 0.5 mL for females), a muscarinic receptor antagonist known to alleviate motion sickness²¹. To account for the effects of the drug, an independent control group of 12 adults (4 female; mean (SD) age 24 (3) years) who received scopolamine was also included. These participants had no previous experience with PFs.

All participants provided a signed informed consent form. The study was approved by the local ethics committee of the Antwerp University Hospital (13/38/357), by the European Space Agency (ESA) medical board and by the Comité de Protection des Personnes Nord Ouest III (Caen, France). All clinical investigations have been conducted according to the principles expressed in the Declaration of Helsinki.

Procedure. The PFs took place during the European Space Agency (ESA) PF campaigns on board of the Airbus A-300 Zero G, in April 2014 (60th campaign) and September 2014 (61st campaign); and on board of the Airbus A-310 Zero G in May 2015 (1st cooperative CNES/DLR/ESA PF campaign) and June 2015 (62th campaign). All flights departed from Bordeaux-Merignac airport (France) and were exploited by Novespace (www.novespace.fr). Each campaign consisted of PFs on 3 consecutive days. Each PF included 31 parabolic manoeuvres

at zero g. Every parabola started with a pull-up phase and ended with a pull-out phase at 1.8 g, both lasting about 20 s. The duration of the zero-g condition was about 21 s (Fig. 1). Every flight lasted approximately three hours in total.

Approximately one hour before take-off, all participants were administered a subcutaneous injection of scopolamine by the campaign medical doctor as is routinely the case in PFs²². On board, subjects were seated and secured with a safety belt during the first 5 parabolas, to enhance adaptation to the peculiar sensation of gravity shifts. Afterwards, they were allowed to free-float in a therefore restricted zone for at least 5 consecutive parabolas. A pre-flight scanning session took place 1 to 2 days before the flight and the post-flight session was performed right after (<4 hours) the completion of the flight, at the University of Bordeaux and University Hospital of Bordeaux (France).

Prior to and immediately after PF, participants fulfilled standardized questionnaires assessing the level of wakefulness, emotional function and motion sickness²³. The Epworth Sleepiness Scale²⁴ (ESS) is a 8-item scale ranging from 0–3, which assesses sleepiness and it was incorporated to assess the possible fatigue and drowsiness associated with the administration of scopolamine; a score of 10 separates between normal individuals and excessive daytime sleepiness. The Positive and Negative Affect Scale (PANAS)²⁵ is a 20-item measure of positive and negative affect ranging from 1 to 5; momentary mean scores for the Positive Affect Score is 29.7 (7.9) and for the Negative Affect Score is 14.8 (5.4). The Motion Sickness Assessment Questionnaire (MSAQ)²⁶ is a 16-item questionnaire comprising of four subscales, all assessing a different aspect of motion sickness (gastrointestinal, central, peripheral and sopite-related). The Misery Scale (MISC)²⁷ is an 11-point scale ranging from 0 to 10 which measures the level of motion sickness; each participant had to report a MISC score 7 times in total: pre-flight (seated in the plane before take-off), after the 1st, 6th, 10th, 20th and 30th parabola and post-flight (right after landing). Questionnaire data were also collected in the scopolamine control group in the same way. Data were analysed with SPSS v21 (IBM Corp, Armonk, New York). Bonferroni-corrected Wilcoxon Signed Rank tests were performed to test differences in scoring between pre- and post PF, as well as between pre- and post- scopolamine intake in the control group.

Data acquisition. PF group: pre- and post-flight data were acquired on a 3 T GE MR 750 W (GE Healthcare, Milwaukee, Wisconsin, USA) MRI scanner at the University of Bordeaux and University Hospital of Bordeaux (France), using a 32-channel head coil. During resting state, 280 multislice T2*-weighted images were acquired with a gradient-echo echo-planar imaging sequence using axial slice orientation and covering the whole brain (voxel size = 3 × 3 × 3 mm; matrix size = 64 × 64 × 42; repetition time = 2 s; echo time = 20 ms; flip angle = 77°; field of view = 192 × 192 mm). For anatomical reference, a high-resolution T1-weighted image was acquired for each subject (T1-weighted 3D magnetization-prepared rapid gradient echo sequence).

Scopolamine control group (non-PF): two scanning sessions took place, a baseline medication-free session and 3 hours after the administration of scopolamine (Antwerp University Hospital, Belgium). Pre- and post-scopolamine data were acquired on a 3 T Siemens MAGNETOM Prisma scanner (Siemens, Erlangen, Germany), using a 32-channel head coil. During the resting state scanning period, an identical MRI sequence was used as for the PF group.

Data analysis. Data preprocessing was performed with Statistical Parametric Mapping 12 (SPM12; www.fil.ion.ucl.ac.uk/spm) and statistical analysis with the CONN v.16 functional connectivity toolbox (www.nitrc.org/projects/conn). The initial three volumes were discarded to avoid T1 saturation effects. Preprocessing steps included slice-time correction, realignment, segmentation of structural data, normalization into standard stereotactic Montreal Neurological Institute (MNI) space and spatial smoothing using a Gaussian kernel of 6 mm full width at half-maximum (FWHM). Motion correction further encompassed motion artifact detection and rejection using the artifact detection toolbox (ART; http://www.nitrc.org/projects/artifact_detect). Specifically, an image was defined as an outlier image if the head displacement in x, y, or z direction was greater than 0.5 mm from the previous frame, or if the rotational displacement was greater than 0.02 radians from the previous frame, or if the global mean intensity in the image was greater than 3 SDs from the mean image intensity for the entire resting session. Outliers in the global mean signal intensity and motion were subsequently included as nuisance regressors within the first-level general linear model. For noise reduction, we used the anatomical component-based noise correction method aCompCor²⁸. This approach models the influence of noise as a voxel-specific linear combination of multiple empirically estimated noise sources by deriving principal components from noise regions of interest (ROIs) and by including them as nuisance parameters within first-level general linear model. Specifically, the anatomical image for each participant was segmented into white matter (WM), gray matter, and cerebrospinal fluid (CSF) masks. To minimize partial voluming with gray matter, the WM and CSF masks were eroded by one voxel, which resulted in substantially smaller masks than the original segmentations²⁹. The eroded WM and CSF masks were then used as noise ROIs. Signals from the WM and CSF noise ROIs were extracted from the unsmoothed functional volumes to avoid additional risk of contaminating WM and CSF signals with gray matter signals. A temporal band-pass filter of 0.008–0.09 Hz was applied. Residual head motion parameters (three rotation and three translation parameters, plus another six parameters representing their first-order temporal derivatives) were also regressed out.

Statistical analysis adopted a hypothesis-free (voxel-to-voxel) approach. First-level voxel-to-voxel analysis encompassed the estimation of voxel-to-voxel functional correlation matrix within each subject. From the residual BOLD time series at every voxel within an a priori GM mask (isotropic 2-mm voxels) the matrix of voxel-to-voxel bivariate correlation coefficients was computed³⁰. From this voxel-to-voxel correlation matrix, the intrinsic connectivity contrast (ICC) was computed³¹. The ICC characterizes the strength of the global connectivity pattern between each voxel and the rest of the brain. In short, the ICC is based on network theory's degree metric, which represents the number of voxels showing a correlation with each other

	Pre flight (n = 24)	During flight* (n = 24)	Post flight (n = 24)	Pre scop (n = 12)	During scop (n = 12)	Post-scop (n = 12)
PANAS, Positive Affect subscale	35 (4)		35 (6)	32 (6)		29 (7)
PANAS, Negative Affect subscale	16 (4)		12 (5)	12 (2)		11 (1)
Epworth Sleepiness Scale	7 (3)		8 (5)	6 (3)		9 (4)
MSAQ, total (in %)			23 (17)			22 (8)
MSAQ, central subscale (in %)			20 (16)			27 (14)
MSAQ, sopite-related subscale (in %)			22 (20)			31 (15)
MSAQ, gastro-intestinal subscale (in %)			29 (27)			17 (7)
MSAQ, peripheral subscale (in %)			20 (18)			15 (6)
Misery Scale score	0.5 (0.8)	1.2 (1.3)	0.5 (0.8)	0.0 (0.0)	1.0 (0.2)	0.5 (0.7)

Table 1. Subjective ratings on the Positive and Negative Affect Scale, the Epworth Sleepiness questionnaire, Motion Sickness Assessment Questionnaire and Misery Scale scores (mean (SD)). MSAQ: Motion Sickness Assessment Questionnaire; PANAS: Positive and Negative Affect Scale; PF: parabolic flight; scop: scopolamine; SD: standard deviation. *Averaged over the 5 assessments during the flight.

voxel. Therefore, a whole-brain map is produced wherein the intensity of each voxel reflects the degree to which that voxel is connected to the rest of the brain. In order to avoid the need of an arbitrary correlation threshold, an ICC power map is finally created representing the average r^2 connectivity of a given voxel and all the other above threshold voxels, with a greater ICC score representing greater average strength of the correlations in a given voxel. This method of hypothesis-free exploration of connectivity changes has been previously employed by others^{7, 31–35}. Second-level group analysis utilized a 2×2 repeated measures design, with “Group” (PF, non-PF) as between-subject factor, further modelling the effect of scanning site, and “Condition” (Pre-flight scan, Post-flight scan) as within-subject factor. To disentangle the effects observed in the PF group as opposed to the effects attributed to scopolamine, a conjunction was carried out between the post-flight decreases in connectivity in the PF as compared to the non-PF group, and the pre-flight compared to post-flight decreases in connectivity in the PF group only, i.e.: [PF > non-PF Pre < Post negative contrast] & [PF Pre < Post negative contrast]. Due to the unbalanced design, two supplementary analyses were performed in order to increase statistical power and ensure validity and interpretation of the results: connectivity analyses with PF participants matched for age and gender to the non-PF group and bootstrapping (Supplementary Material).

As the ICC is an explorative metric which localizes changes in functional connectivity related to the experimental modulations, classic region of interest-based fMRI connectivity analysis on the regions exhibiting changes was performed to understand the networks associated with the identified nodes³¹. For these seed regions, time-series from the contained voxels were averaged together. This averaged time-series was used to estimate whole-brain correlation r maps, which were then converted to normally distributed Fisher’s z transformed correlation maps to allow for subsequent group-level analysis. Non-parametric permutation tests assessed the distributions of each experimental group or condition.

Results

Questionnaires. Out of the 28 included participants, 24 fulfilled the PANAS, ESS, MSAQ and MISC questionnaires. Data from 4 participants was not assessed due to logistical reasons. Based on the self-reports, participants did not experience severe motion sickness, abnormal positive/negative affect or sleepiness (Table 1). After the PF, there was a decrease in negative affect (PANAS subscale) compared to preflight ($Z = -3.99$, $p < 0.001$). For the PANAS positive affect and the ESS, there were no differences. After scopolamine intake, there was a decrease in positive affect (PANAS subscale) compared to pre-scopolamine ($Z = -2.606$, $p = 0.009$). No differences were found for the PANAS negative affect subscale and the ESS questionnaire.

Connectivity analysis. In terms of motion, four outlier images were detected in the PF group and none in the non-PF group. For the ICC explorative analysis, the main effects of each group at pre- and post-scan are summarized in Fig. 2. For the PF group, between-condition differences were identified in posterior cingulate cortex and right parietal gyrus. For the non-PF group, no post-pre scan differences in ICC connectivity were found (Fig. 3). The interaction analysis revealed that the modification of the connectivity pattern was observed in the right temporo-parietal junction (rTPJ)/angular gyrus (rAG) in the PF group in comparison to the non-PF group, at post-scan as compared to pre-scan assessment ($T(38) = -3.32$, $p < 0.001$ FWE cluster-level, permutation testing; cluster size: 260 voxels, peak coordinate $x, y, z = [58-64 18]$). The rAG was also identified after the conjunction analysis (cluster size: 148 voxels, $x, y, z = [57-66 25]$; Fig. 3), and the two sub-analyses with the age and gender-matched groups and bootstrapping (Supplementary Material).

The rAG identified by the interaction analysis was then used as a seed area to perform classic region of interest analysis in order to better comprehend the network associated with the identified node. Both in pre-flight and post-flight scan the encompassed areas showing positive connectivity were located in lateral parietal, superior/middle frontal gyri, superior/middle/inferior temporal gyri as well as mesio-frontal, posterior parietal/precuneal regions and cerebellum. Negative connectivity was identified in bilateral supramarginal gyri/SMA, superior frontal gyri and temporal/temporo-occipital/lateral occipital regions (Fig. 4). Between-condition contrast pointed to

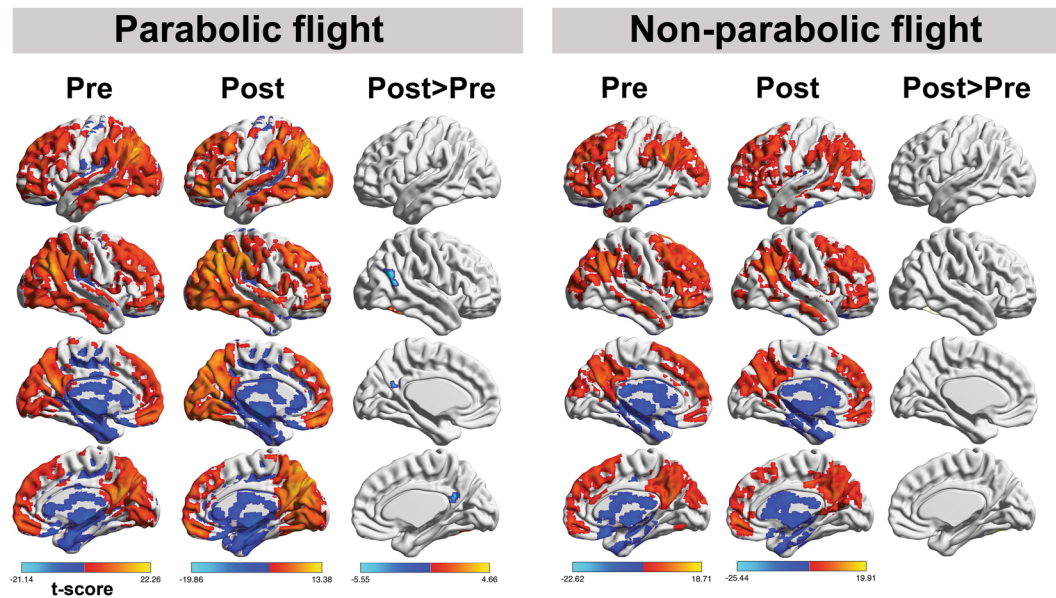


Figure 2. Group-level explorative analysis was performed to localize modifications in global connectivity before and after participation to the parabolic flight ($n = 28$) and before and after scopolamine intake in the non-parabolic flight group ($n = 12$). The spatial patterns represent average maps of higher (red) and lower (blue) intrinsic connectivity contrast scores, with a greater score representing greater average strength of the correlations in a given voxel. Statistical maps are rendered on a surface template and are thresholded at cluster-level family wise error rate $p < 0.05$ (two-sided, permutation testing).

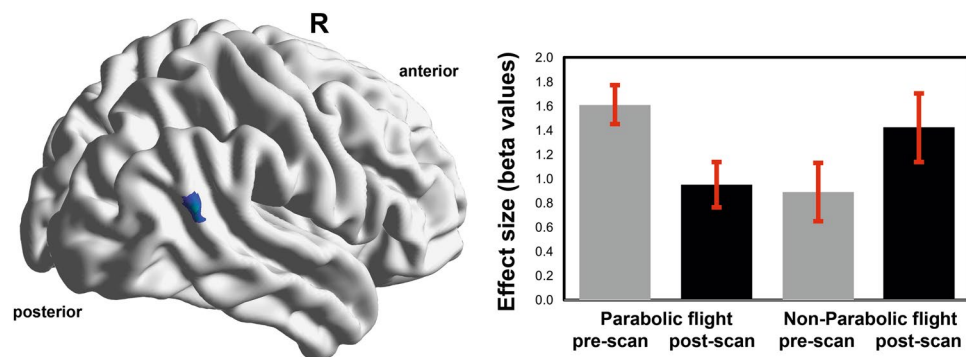


Figure 3. The hypothesis-free exploration of connectivity changes points to the right angular gyrus/temporo-parietal junction as the region with lower scores on the intrinsic connectivity contract, implying that this region has decreased participation in whole-brain connectivity at post-flight scan. The map represents the results of the conjunction analysis, suggesting that the effect can be attributed to the parabolic flight group as compared to the non-parabolic flight control group. Bars indicate effect sizes (beta values) and error bars 90% CI in the same cluster.

fewer negative correlations (anticorrelations) with R supramarginal (SMG; BA 40; 63–24 31) and L supramarginal gyri (SMG; BA 40; –59–31 36) (FWE $p < 0.05$ cluster-level, permutation testing) at post- compared to pre-flight scan.

Discussion

The aim of the present study was to assess functional connectivity changes after short-term acute exposure to gravitational alterations. Hereto, we exposed healthy naïve individuals to a PF and measured resting-state fMRI connectivity before and after the exposure to altered gravitational forces. With no a priori assumptions, we found a decrease of the ICC scores in the rTPJ/rAG after the PF. These results suggest the rAG/TPG has reduced participation in whole-brain connectivity after short-term exposure to altered gravity, most possibly related to changes in vestibular function. For instance, in order to maintain gaze stabilization, postural control and spatial orientation, the human brain integrates visual, somatosensory and vestibular input signals³⁶. In the vestibular system, angular accelerations are detected by the semicircular canals, while linear accelerations, and thus gravity, are sensed by the otolith organs (i.e. utricle and saccule). Therefore, due to the alterations in gravitational force,

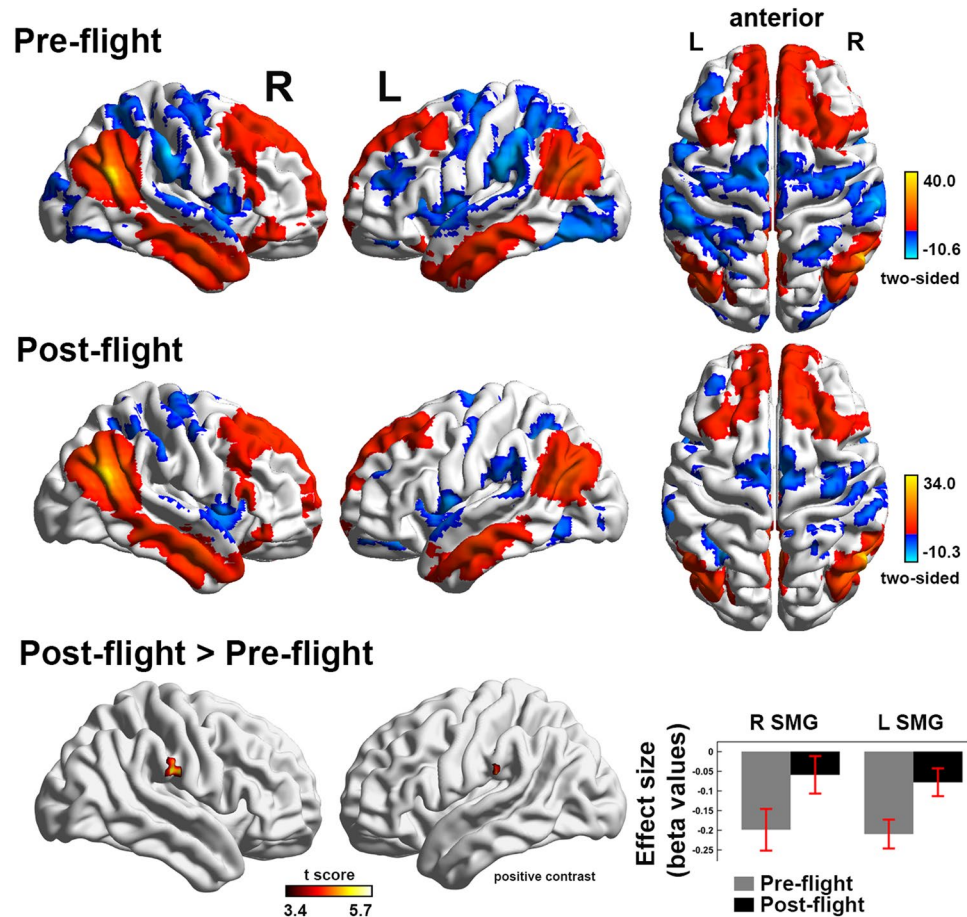


Figure 4. The networks encompassed by the right angular gyrus/temporo-parietal junction in the parabolic flight group. The default mode network (DMN; red) and the DMN anticorrelated regions (blue) were the set of areas that were functionally connected with the right angular gyrus at pre- and post-flight. The between-condition differences in the encompassed networks included fewer anticorrelations with bilateral supramarginal gyri. The statistical maps are rendered on a surface template and have been thresholded at cluster-level family wise error rate $p < 0.05$ (permutation tests). Bars indicate cluster-level effect sizes (beta values) and error bars 90% CI.

the afferent information from the otolith organs is significantly altered. This gives rise to a loss of congruence between visual, proprioceptive and vestibular input and the loss of the otherwise tight coupling of canal-otolith information in the presence of Earth's gravity. As a result, the vestibular system and its functions are challenged thoroughly.

Previous investigations also suggest that the rAG is involved in the processing and integration of vestibular, visual and proprioceptive input³⁷. For example, inhibition of the right TPJ caused difficulties with the perception of the upright and maintaining an internal representation of verticality^{38, 39}. Also, disruptive TMS to the AG showed that this region mediated the interaction between visuo-proprioceptive weighting and realignment⁴⁰. Past studies further point to the involvement of the TPJ in timing of interception of an object⁴¹. With regards to the effects of gravity, it was found that the attempt to intercept an object accelerated by gravity had a reverse response pattern in weightlessness as compared to normal gravity^{42, 43}. In the same line, an fMRI study, assessing the perception of moving objects according to natural or reversed gravity, found the engagement of the TPJ and insula, suggesting an internalization of gravity in these regions⁴⁴. Indeed, when a sensory mismatch occurs, e.g. between proprioceptive and visual information, the brain can rearrange the two modalities, by calibrating the modality which receives the lowest weight⁴⁵. The correlation between the weight of a modality and the extent of calibration during a mismatch was found to be disrupted when TMS temporarily inactivated the AG⁴⁰. Taken together, these studies suggest an important role of the TPJ in the integration of multisensory modalities for achieving optimal vestibular function. During a PF, there is a constant shift in gravity levels provoking many conflicting sensory signals, such as proprioception^{10, 46}. The latter occurs in combination with visual disturbed impressions when floating upside down during the microgravity phase. This can hamper verticality and perception of self-location^{47–50}.

Important as the rAG may be for vestibular processing, it is commonly accepted that the human brain does not possess a unique primary vestibular cortex and that vestibular information is processed in a distributed network (e.g. refs 51 and 52). From electrophysiological and tracer studies in primates, as well as neuroimaging

studies in humans, we know that the so-called “vestibular cortex” encompasses the TPJ and posterior insula, the somatosensory cortex, the posterior parietal cortex, the anterior insula, and the lateral and medial frontal cortices⁵³. Specifically, the parieto-insular vestibular cortex (PIVC) in primates is considered as the “hot spot” of vestibular processing^{51, 52} which presumably maps to the parietal operculum (OP2) in humans⁵⁴. However, the exact location of the human analogue of the PIVC remains controversial⁵¹. The fact that this key region was not identified in our analysis can only be speculated. Future hypothesis-driven explorations of the vestibular cortex may shed more light on the preferential contribution of each region to the PF experience.

Interestingly, the TPJ has been considered important for bodily self-consciousness^{50, 55}, i.e., the non-conceptual and pre-reflective processing and representation of body-related information⁵⁶. With regards to self-location (“where I am in space”), previous studies with patients with epileptic seizures and focal electrical stimulation of the TPJ elicited sensations of body tilt and altered gravity. Interestingly, the AG and TPJ have been reported to be involved in out-of-body experiences, which can be considered as a deficient perception of self-location and self-being, when this area is inactivated or lesioned^{49, 57–61}. Furthermore, reports from people experiencing microgravity (either during a PF or during spaceflight) have elucidated that the absence of gravity can elicit several illusory own-body perceptions, e.g. the inversion illusion (i.e. the feeling of the body being upside-down relative to the extrapersonal space or vice versa)⁶². Such experience is considered to be the result of a combination of altered gravitational input, a multisensory disintegration and top-down modulation⁵⁵. Considering the above, it is possible that the here identified reduced rAG connectivity implies the inability to compute and correct the conflicting sensory inputs it receives during microgravity.

Our results also resonate with lesion studies, pointing to the right hemisphere for elaborating an internal model of verticality and controlling body orientation⁶³. For example, patients with Pusher syndrome (a disorder of postural balance that manifests as a pushing away toward the contralesional side in unilateral stroke) were shown to depend predominantly on otolith inputs when they sustained right hemispheric lesions⁴⁷. This indicates an asymmetrical otolith mechanism, concurrent with a dominance of the right non-dominant hemisphere in processing vestibular cues⁶⁴. Also, a PET study in patients with a unilateral vestibular neuritis showed that the vestibular graviceptive deficits in these patients (as measured by the deviation on the subjective visual vertical) correlate positively with regional glucose metabolism in the right hemisphere⁶⁵. This highlights not only the lateralized dominance of the cortical vestibular network, but also the functional dominance in verticality perception and the processing of gravitational cues, resonating with our findings.

We also found decreases in the anticorrelated connectivity between the rAG/rTPJ and bilateral SMG after the flight. Anatomically, the AG and SMG are connected through arcuate (u-shaped) connections within the same hemisphere⁶⁶. The SMG plays a well-established role in vestibular function, as shown by studies implementing both caloric^{44, 64, 67–70} and galvanic vestibular stimulation^{71, 72}. Additionally, the SMG plays a distinct role in the perception of verticality³⁸. Apart from this within-hemispheric connection, there is both a structural and functional interhemispheric connectivity between the AG and SMG⁷³. Interestingly, the rAG is part of the default mode network (DMN) while the SMG are part of a set of areas classically anticorrelating to the DMN^{74, 75}. Such anticorrelated connectivity has been associated with cognitive function^{76–79} and seems to mediate the level of consciousness^{80, 81}. In short, stronger anticorrelations are thought to reflect a more effective capacity to switch between internal and external modes of attention⁸², with a self-related counterpart⁸³. Therefore, the here-identified reductions in the anticorrelations may suggest a reduced ability for self-related monitoring during weightlessness.

It is possible that the observed changes in functional connectivity are due to a discrepancy between the gravitational vertical, as determined by integrated sensory information, and the expected vertical based on previous experience⁸⁴. Such differences in experienced and expected spatial representations have also been estimated in off-vertical axis rotation⁸⁵ and tilting train studies⁸⁶. However, it remains challenging whether the observed effects can be attributed to microgravity, hypergravity or to the general transitions of the gravitational force, which are all induced during PF. With the current setup, we are unable to make specific assumptions as to the origin of the effect. Our control group did not engage in an activity that could mimic the characteristics of the PF, i.e. the alternation between the absence of gravity and the presence of hypergravity. Hence, we could not obtain a highly-controlled environment for the PF participants. Designs controlling for the effect of microgravity and the exposure to hypergravity, which is approximately twice the length of that spent in microgravity, might be able to disentangle between the effects of these two forces in the human brain. Finally, a potential confounder could be the mismatch in the time interval between scopolamine injection and post-scan sessions, which was on average 6 h for the PF group and 3 h for the non-PF group. We believe that this difference in scanning interval does not pose an issue on our analysis. This is because of the low dose of injected scopolamine in the non-PF group (0.175 mg for males, 0.125 mg for females), which was expected to washout after the 3 h interval. Based on a previous study assessing the effect of subcutaneous scopolamine (0.4 mg, 0.6 mg and 0.8 mg) on psychomotor tests, it was shown that scopolamine negatively affected the tests with a peak between 1–2 h after administration; after 3 h, values returned to baseline⁸⁷. Here, the fact that we did not identify connectivity differences in the non-PF group between the post-pre scans, suggests a satisfactory baseline assessment for the PF group. Other fMRI studies, however, show that scopolamine affects functional connectivity^{88–91}. In light of the different scanning setup, different dosage and administration type, it seems that results are not conclusive as to the exact affected regions. Also, even with scopolamine, motion sickness during PFs can still be present^{23, 92}. Here, PF participants showed relatively low motion sickness scores. Additionally, they reported decreases in the negative affect as measured on subscale of the PANAS questionnaire after PF. This effect can be related to the fact that participants were generally excited by experiencing weightlessness. At the same time, we found a decrease in positive affect in the control group, which could be possibly related to boredom as reported in a previous study⁹³. These confounds as well as the fact that a PF is associated with high stress levels and increases in stress hormones^{94–96} should be taken into consideration by future investigations.

In conclusion, we found that exposure to short-term acute alterations of gravity induced by a PF led to decreased intrinsic connectivity strength in the rAG/rTPJ, a region known to be involved in multisensory integration, cognitive and spatial tasks. Decreases in short-distance (within-hemisphere) and long-distance (inter-hemispheric) anticorrelations between the rAG/rTPJ and bilateral SMG were further identified. These results are relevant for long-duration spaceflight, as well as for space tourism, where less-trained humans will be exposed to similar and even more extreme gravitational transitions. Taken together, our findings shed light not only on the understanding of how the brain is affected by short-term alteration of gravitational input and the internalization of gravity in the human brain, but are also relevant for the understanding of bodily self-consciousness.

References

- Clément, G. *Fundamentals of Space Medicine*. (Springer, 2011).
- Lackner, J. R. & DiZio, P. Space motion sickness. *Experimental Brain Research* **175**, 377–399 (2006).
- Holstein, G. R., Kukielka, E. & Martinelli, G. P. Anatomical observations of the rat cerebellar nodulus after 24 hr of spaceflight. *J. Gravit. Physiol.* **6**, P47–P50 (1999).
- Newberg, A. B. Changes in the central nervous system and their clinical correlates during long-term spaceflight. *Aviat. Space. Environ. Med.* **65**, 562–572 (1994).
- Ross, M. D. A spaceflight study of synaptic plasticity in adult rat vestibular maculas. *Acta Otolaryngol. Suppl.* **516**, 1–14 (1994).
- Van Ombergen, A. *et al.* Spaceflight-induced neuroplasticity in humans as measured by MRI: what do we know so far? *npj Microgravity* **3** (2017).
- Demertzi, A. *et al.* Cortical reorganization in an astronaut's brain after long-duration spaceflight. *Brain Struct. Funct.* **221**, 2873–2876 (2016).
- Navasiolava, N. M. *et al.* Long-term dry immersion: Review and prospects. *Eur. J. Appl. Physiol.* **111**, 1235–1260 (2011).
- Pavy-Le Traon, A., Heer, M., Narici, M. V., Rittweger, J. & Vernikos, J. From space to Earth: Advances in human physiology from 20 years of bed rest studies (1986–2006). *European Journal of Applied Physiology* **101** (2007).
- Karmali, F. & Shelhamer, M. The dynamics of parabolic flight: Flight characteristics and passenger percepts. *Acta Astronaut* **63**, 594–602 (2008).
- lv, B., Shao, Q., Chen, Z., Ma, L. & Wu, T. Effects of acute electromagnetic fields exposure on the interhemispheric homotopic functional connectivity during resting state. In *Proceedings of the Annual International Conference of the IEEE Engineering in Medicine and Biology Society, EMBS*. **2015**–Novem, 1813–1816 (2015).
- Hermans, E., Henckens, M., Joels, M. & Fernandez, G. Dynamic adaptation of large-scale brain networks in response to acute stressors. *Trends Neurosci.* **37**, 304–314 (2014).
- van Marle, H., Hermans, E., Qin, S. & Fernandez, G. Enhanced resting-state connectivity of amygdala in the immediate aftermath of acute psychological stress. *Neuroimage* **53**, 348–354 (2010).
- Tagliazucchi, E. *et al.* Increased Global Functional Connectivity Correlates with LSD-Induced Ego Dissolution. *Curr. Biol.* **26**, 1043–1050 (2016).
- Carhart-Harris, R. L. *et al.* Neural correlates of the psychedelic state as determined by fMRI studies with psilocybin. *Proc. Natl. Acad. Sci. USA* **109**, 2138–43 (2012).
- Lopez, C., Bachofner, C., Mercier, M. & Blanke, O. Gravity and observer's body orientation influence the visual perception of human body postures. *J. Vis.* **9**(1), 1–14 (2009).
- Lackner, J. R. & DiZio, P. Multisensory, cognitive, and motor influences on human spatial orientation in weightlessness. *J. Vestib Res* **3**, 361–372 (1993).
- Van Ombergen, A. *et al.* The effect of spaceflight and microgravity on the human brain. *J. Neurol.* In print (2017).
- Newberg, A. B. & Alavi, A. Changes in the central nervous system during long-duration space flight: implications for neuroimaging. *Adv. Space Res.* **22**, 185–196 (1998).
- Biswal, B. B., Van Kylen, J. & Hyde, J. S. Simultaneous assessment of flow and BOLD signals in resting-state functional connectivity maps. *NMR Biomed.* **10**, 165–170 (1997).
- Lochner, M. & Thompson, A. J. The muscarinic antagonists scopolamine and atropine are competitive antagonists at 5-HT₃ receptors. *Neuropharmacology* **108**, 220–228 (2016).
- Wood, C. D., Manno, J. E., Manno, B. R., Odenheimer, R. C. & Bairnsfather, L. E. The effect of antimotion sickness drugs on habituation to motion. *Aviat. Sp. Environ. Med* **57**, 539–542 (1986).
- Van Ombergen, A., Lawson, B. D. & Wuyts, F. L. Motion sickness and sopite syndrome associated with parabolic flights: a case report. *Int J Audiol* **55**, 189–94 (2016).
- Johns, M. W. A new method for measuring daytime sleepiness: the Epworth sleepiness scale. *Sleep* **14**, 540–545 (1991).
- Watson, D., Clark, L. A. & Tellegen, A. Development and validation of brief measures of positive and negative affect: the PANAS scales. *J. Pers. Soc. Psychol.* **54**, 1063–1070 (1988).
- Gianaros, P. & Muth, E. A questionnaire for the assessment of the multiple dimensions of motion sickness. *Aviat. Sp. Environ. Med* **72**, 115–119 (2001).
- Bos, J. E., MacKinnon, S. N. & Patterson, A. Motion sickness symptoms in a ship motion simulator: Effects of inside, outside, and no view. *Aviat. Sp. Environ. Med* **76**, 1111–1118 (2005).
- Behzadi, Y., Restom, K., Liu, J. & Liu, T. T. A component based noise correction method (CompCor) for BOLD and perfusion based fMRI. *Neuroimage* **37**, 90–101 (2007).
- Chai, X. J., Castañán, A. N., Öngür, D. & Whitfield-Gabrieli, S. Anticorrelations in resting state networks without global signal regression. *Neuroimage* **59**, 1420–1428 (2012).
- Raichle, M. The restless brain. *Brain Connect* **1**, 3–12 (2011).
- Martuzzi, R. *et al.* A whole-brain voxel based measure of intrinsic connectivity contrast reveals local changes in tissue connectivity with anesthetic without a priori assumptions on thresholds or regions of interest. *Neuroimage* **58**, 1044–1050 (2011).
- Vatansver, D., Manktelow, A. E., Sahakian, B. J., Menon, D. K. & Stamatakis, E. A. Angular default mode network connectivity across working memory load. *Hum. Brain Mapp*, doi:10.1002/hbm.23341 (2016).
- Pravatà, E. *et al.* Hyperconnectivity of the dorsolateral prefrontal cortex following mental effort in multiple sclerosis patients with cognitive fatigue. *Mult. Scler. J*, doi:10.1177/1352458515625806 (2016).
- Muller, A. M., Méritat, S. & Jäncke, L. Older but still fluent? Insights from the intrinsically active baseline configuration of the aging brain using a data driven graph-theoretical approach. *Neuroimage* **127**, 346–362 (2016).
- Layden, E. A. *et al.* Perceived social isolation is associated with altered functional connectivity in neural networks associated with tonic alertness and executive control. *Neuroimage*, doi:10.1016/j.neuroimage.2016.09.050 (2016).
- Goldberg, J. M. *et al.* The Vestibular System: A Sixth Sense. *The Vestibular System: A Sixth Sense*, doi:10.1093/acprof:oso/9780195167085.001.0001 (2012).
- Besnard, S., Lopez, C., Brandt, T., Denise, P. & Smith, P. F. *The Vestibular System in Cognitive and Memory Processes in Mammals*. (Frontiers Media SA, 2016).

38. Kheradmand, A., Lasker, A. & Zee, D. S. Transcranial magnetic stimulation (TMS) of the supramarginal gyrus: A window to perception of upright. *Cereb. Cortex* **25**, 765–771 (2015).
39. Fiori, F., Candidi, M., Acciarino, A., David, N. & Aglioti, S. M. The right temporo parietal junction plays a causal role in maintaining the internal representation of verticality. *J. Neurophysiol.* **3**, jn.00289.2015 (2015).
40. Block, H., Bastian, A. & Celnik, P. Virtual lesion of angular gyrus disrupts the relationship between visuoproprioceptive weighting and realignment. *J. Cogn. Neurosci.* **25**, 636–48 (2013).
41. Bosco, G., Carrozzo, M. & Lacquaniti, F. Contributions of the human temporo-parietal junction and MT/V5+ to the timing of interception revealed by TMS. *J. Neurosci.* **28**, 12071–12084 (2008).
42. Senot, P., Zago, M., Lacquaniti, F. & McIntyre, J. Anticipating the effects of gravity when intercepting moving objects: differentiating up and down based on nonvisual cues. *J. Neurophysiol.* **94**, 4471–4480 (2005).
43. Senot, P. *et al.* When Up Is Down in 0g: How Gravity Sensing Affects the Timing of Interceptive Actions. *J. Neurosci.* **32**, 1969–1973 (2012).
44. Indovina, I. *et al.* Representation of visual gravitational motion in the human vestibular cortex. *Science (80-)* **208**, 416–9 (2005).
45. Block, H. J. & Bastian, A. J. Sensory weighting and realignment: independent compensatory processes. *J. Neurophysiol.* **106**, 59–70 (2011).
46. Roll, R. *et al.* Proprioceptive information processing in weightlessness. *Exp. Brain Res.* **122**, 393–402 (1998).
47. Baier, B., Suchan, J., Karnath, H. O. & Dieterich, M. Neural correlates of disturbed perception of verticality. *Neurology* **78**, 728–735 (2012).
48. Barra, J. *et al.* Humans use internal models to construct and update a sense of verticality. *Brain a J. Neurol.* **133**, 3552–3563 (2010).
49. Ionta, S. *et al.* Multisensory Mechanisms in Temporo-Parietal Cortex Support Self-Location and First-Person Perspective. *Neuron* **70**, 363–374 (2011).
50. Pfeiffer, C., Serino, A. & Blanke, O. The vestibular system: a spatial reference for bodily self-consciousness. *Frontiers in Integrative Neuroscience* **8**, 31 (2014).
51. Lopez, C., Blanke, O. & Mast, F. The vestibular cortex in the human brain revealed by coordinate-based activation likelihood estimation meta-analysis. *Neuroscience* **60**, 162–169 (2012).
52. Zu Eulenburg, P., Caspers, S., Roski, C. & Eickhoff, S. B. Meta-analytical definition and functional connectivity of the human vestibular cortex. *Neuroimage* **60**, 162–169 (2012).
53. Guldin, W. O. & Grüsser, O. J. Is there a vestibular cortex? *Trends in Neurosciences* **21**, 254–259 (1998).
54. Eickhoff, S., Amunts, K., Mohlberg, H. & Zilles, K. The Human parietal operculum. II. Stereotaxic maps and correlation with functional imaging results. *Cereb. Cortex* **16**, 268–279 (2006).
55. Blanke, O. Multisensory brain mechanisms of bodily self-consciousness. *Nat. Rev. Neurosci.* **13**, 556–71 (2012).
56. Gallagher, S. Philosophical conceptions of the self: Implications for cognitive science. *Trends in Cognitive Sciences* **4**, 14–21 (2000).
57. Isnard, J., Guénot, M., Sindou, M. & Mauguière, F. Clinical Manifestations of Insular Lobe Seizures: A Stereo-electroencephalographic Study. *Epilepsia* **45**, 1079–1090 (2004).
58. Nguyen, D. K. *et al.* Revisiting the role of the insula in refractory partial epilepsy. *Epilepsia* **50**, 510–520 (2009).
59. Heydrich, L., Lopez, C., Seeck, M. & Blanke, O. Partial and full own-body illusions of epileptic origin in a child with right temporoparietal epilepsy. *Epilepsy Behav.* **20**, 583–586 (2011).
60. Blanke, O., Ortigue, S., Landis, T. & Seeck, M. Stimulating illusory own-body perceptions. *Nature* **419**, 269–270 (2002).
61. De Ridder, D., Van Laere, K., Dupont, P., Menovsky, T. & Van de Heyning, P. Visualizing out-of-body experience in the brain. *N. Engl. J. Med.* **357**, 1829–1833 (2007).
62. Graybiel, A. & Kellogg, R. The inversion illusion in parabolic flight: its probable dependence on otolith function. *Aerosp. Med* **38**, 1099–1103 (1967).
63. Pérennou, D. A. *et al.* Lateropulsion, pushing and verticality perception in hemisphere stroke: A causal relationship? *Brain* **131**, 2401–2413 (2008).
64. Dieterich, M. *et al.* Dominance for vestibular cortical function in the non-dominant hemisphere. *Cereb. Cortex* **13**, 994–1007 (2003).
65. Bense, S. *et al.* Metabolic changes in vestibular and visual cortices in acute vestibular neuritis. *Ann. Neurol.* **56**, 624–630 (2004).
66. Lee, H. *et al.* Anatomical traces of vocabulary acquisition in the adolescent brain. *J. Neurosci.* **27**, 1184–9 (2007).
67. Bottini, G. *et al.* Identification of the central vestibular projections in man: a positron emission tomography activation study. *Exp. Brain Res.* **99**, 164–169 (1994).
68. Vitte, E. *et al.* Activation of the hippocampal formation by vestibular stimulation: a functional magnetic resonance imaging study. *Exp. Brain Res.* **112**, 523–6 (1996).
69. Suzuki, M. *et al.* Cortical and subcortical vestibular response to caloric stimulation detected by functional magnetic resonance imaging. *Cogn. Brain Res.* **12**, 441–449 (2001).
70. Deutschländer, A. *et al.* Sensory system interactions during simultaneous vestibular and visual stimulation in PET. *Hum. Brain Mapp.* **16**, 92–103 (2002).
71. Bense, S., Stephan, T., Yousry, T. a., Brandt, T. & Dieterich, M. Multisensory cortical signal increases and decreases during vestibular galvanic stimulation (fMRI). *J. Neurophysiol.* **85**, 886–899 (2001).
72. Stephan, T. *et al.* Functional MRI of galvanic vestibular stimulation with alternating currents at different frequencies. *Neuroimage* **26**, 721–732 (2005).
73. Uddin, L. Q. *et al.* Dissociable connectivity within human angular gyrus and intraparietal sulcus: Evidence from functional and structural connectivity. *Cereb. Cortex* **20**, 2636–2646 (2010).
74. Fox, M. D. *et al.* The human brain is intrinsically organized into dynamic, anticorrelated functional networks (2005).
75. Fransson, P. Spontaneous low-frequency BOLD signal fluctuations: An fMRI investigation of the resting-state default mode of brain function hypothesis. *Hum. Brain Mapp.* **26**, 15–29 (2005).
76. Whitfield-Gabrieli, S. *et al.* Hyperactivity and hyperconnectivity of the default network in schizophrenia and in first-degree relatives of persons with schizophrenia. *Proc. Natl. Acad. Sci. USA* **106**, 1279–84 (2009).
77. Vanhaudenhuyse, A. *et al.* Two distinct neuronal networks mediate the awareness of environment and of self. *J. Cogn. Neurosci.* **23**, 570–578 (2011).
78. Demertzi, A., Soddu, A., Faymonville, M., Bahri, M. A. & Gosseries, O. Hypnotic modulation of resting state fMRI default mode and extrinsic network connectivity. *Slow Brain Oscillations of Sleep Resting State and Vigilance* **193**, (Elsevier B. V., 2011).
79. Keller, J. B. *et al.* Resting-state anticorrelations between medial and lateral prefrontal cortex: Association with working memory, aging, and individual differences. *Cortex* **64**, 271–280 (2015).
80. Di Perri, C. *et al.* Neural correlates of consciousness in patients who have emerged from a minimally conscious state: A cross-sectional multimodal imaging study. *Lancet Neurol.* **15**, 830–42 (2016).
81. Demertzi, A., Soddu, A. & Laureys, S. Consciousness supporting networks. *Curr Opin Neurobiol* **23**, 239–244 (2013).
82. Demertzi, A. & Whitfield-Gabrieli, S. In *The Neurology of Consciousness* 95–105 (Elsevier, 2016), doi:10.1016/B978-0-12-800948-2.00006-6.
83. Demertzi, A. *et al.* Looking for the self in pathological unconsciousness. *Front. Hum. Neurosci.* **7**, 1–6 (2013).
84. Bos, J. E. & Bles, W. Modelling motion sickness and subjective vertical mismatch detailed for vertical motions. *Brain Res. Bull.* **47**, 537–542 (1998).
85. Denise, P., Darlot, C., Droulez, J., Cohen, B. & Berthoz, A. Motion perceptions induced by off-vertical axis rotation (OVAR) at small angles of tilt. *Exp Brain Res* **73**, 106–114 (1988).

86. Neimer, J., Eskiüzümlü, S., Dominey-Ventre, J. & Darlot, C. Trains with a view to sickness. *Curr Biol* **11**, R549–R550 (2001).
87. Ebert, U., Siepmann, M., Oertel, R., Wesnes, K. A. & Kirch, W. Pharmacokinetics and pharmacodynamics of scopolamine after subcutaneous administration. *J. Clin. Pharmacol.* **38**, 720–726 (1998).
88. Sperling, R. *et al.* Functional MRI detection of pharmacologically induced memory impairment. *Proc Natl Acad Sci USA* **99**, 455–460 (2002).
89. Schon, K. *et al.* Scopolamine reduces persistent activity related to long-term encoding in the parahippocampal gyrus during delayed matching in humans. *J. Neurosci.* **25**, 9112–23 (2005).
90. Voss, B. *et al.* Cholinergic blockade under working memory demands encountered by increased rehearsal strategies: Evidence from fMRI in healthy subjects. *Eur. Arch. Psychiatry Clin. Neurosci.* **262**, 329–339 (2012).
91. Shah, D. *et al.* Acute modulation of the cholinergic system in the mouse brain detected by pharmacological resting-state functional MRI. *Neuroimage* **109**, 151–159 (2015).
92. Lackner, J. R. Motion sickness: More than nausea and vomiting. *Experimental Brain Research* **232**, 2493–2510 (2014).
93. Alda, M. *et al.* Validation of the Spanish version of the Multidimensional State Boredom Scale (MSBS). *Health Qual. Life Outcomes* **13**, 59 (2015).
94. Schneider, S. *et al.* Parabolic flight experience is related to increased release of stress hormones. *Eur. J. Appl. Physiol.* **100**, 301–308 (2007).
95. Schneider, S. *et al.* The effect of parabolic flight on perceived physical, motivational and psychological state in men and women: correlation with neuroendocrine stress parameters and electrocortical activity. *Stress* **12**, 336–349 (2009).
96. Strewé, C. *et al.* Effects of parabolic flight and spaceflight on the endocannabinoid system in humans. *Rev. Neurosci.* **23**, 673–680 (2012).

Acknowledgements

We wish to express our gratitude to the staff of CHU Pellegrin Department of Radiology for their participation in this study and their flexibility and effort. We also wish to thank Vladimir Pletser (Chinese Academy of Sciences, former ESA), Alexandra Jaquemet (Novespace), Frédéric Gai (Novespace) & Pierre Denise (University of Caen) for their assistance and expertise in the preparation of the parabolic flight campaigns. Also, we would like to thank Dr. Enzo Tagliazucchi (Institut du Cerveau et de la Moelle Epinière – ICM, Paris, France) and Federico Raimondo, MSc (Department of Computer Science, University of Buenos Aires, Argentina) for methods consultation and code sharing. This work was supported by the European Space Agency (ESA) and BELSPO Prodex, the University and University Hospital of Antwerp, the University and University Hospital of Liège, the French Speaking Community Concerted Research Action, the Research Foundation Flanders (FWO Vlaanderen) the Belgian National Funds for Scientific Research (FRS-FNRS), the Wallonie-Bruxelles International, the James McDonnell Foundation, IAP research network P7/06 of the Belgian Government (Belgian Science Policy), the European Commission, the Public Utility Foundation ‘Université Européenne du Travail’, ‘Fondazione Europea di Ricerca Biomedica’, the Bial Foundation, the Human Brain Project (EU-H2020-FETFLAGSHIP-HBP-SGA1-GA720270) and the LUMINOUS project (EU-H2020-FETOPEN-GA686764). A.V.O. is a Research Fellow of the Research Foundation Flanders (Belgium, FWO Vlaanderen), B.J. is Postdoctoral Fellow at FWO Vlaanderen, A.D. is Postdoctoral Fellow at FRS-FNRS, S.L. is Research Director at FRS-FNRS.

Author Contributions

A.V.O., F.W., B.J., J.S., P.M.P., S.S., P.H.V.D.H., S.L. and A.D. contributed to the conception and design of the study. A.V.O., F.W., B.J., S.J., F.V. and V.D. collected data for the study. A.V.O., F.W., S.L. and A.D. are responsible for data analysis and wrote the main manuscript. All authors interpreted the data and reviewed and approved the manuscript.

Additional Information

Supplementary information accompanies this paper at doi:10.1038/s41598-017-03170-5

Competing Interests: The authors declare that they have no competing interests.

Publisher's note: Springer Nature remains neutral with regard to jurisdictional claims in published maps and institutional affiliations.



Open Access This article is licensed under a Creative Commons Attribution 4.0 International License, which permits use, sharing, adaptation, distribution and reproduction in any medium or format, as long as you give appropriate credit to the original author(s) and the source, provide a link to the Creative Commons license, and indicate if changes were made. The images or other third party material in this article are included in the article's Creative Commons license, unless indicated otherwise in a credit line to the material. If material is not included in the article's Creative Commons license and your intended use is not permitted by statutory regulation or exceeds the permitted use, you will need to obtain permission directly from the copyright holder. To view a copy of this license, visit <http://creativecommons.org/licenses/by/4.0/>.

© The Author(s) 2017